Preparation and Characterization of Nanopigment-Poly(styrene-*co*-*n*-butyl acrylate-*co*-methacrylic acid) Composite Particles by High Speed Homogenization-Assisted Suspension Polymerization

Hendri Widiyandari, Ferry Iskandar, Nobuhiro Hagura, Kikuo Okuyama

Department of Chemical Engineering, Graduate School of Engineering, Hiroshima University, 1-4-1 Kagamiyama, Higashi Hiroshima 739-8527, Japan

Received 9 May 2007; accepted 23 November 2007
DOI 10.1002/app.27814
Published online 23 January 2008 in Wiley InterScience (www.interscience.wiley.com).

ABSTRACT: Composite particles of nanoblue pigment-poly(styrene-*co*-*n*-butyl acrylate-*co*-methacrylic acid) of controllable size were successfully prepared using high-speed homogenization-assisted suspension polymerization. This composite has potential application as a toner for high-resolution printing. A nanosized hybrid blue pigment, with a monodispersed and uniform spherical shape, was employed for the production of composite particles. The effects of agitation speed, pigment concentration, and anionic surfactant concentration on the properties of the prepared composite particles were investigated. Agitation speed plays an important role in controlling particle size. The prepared composite particles have geometric mean diameters in the range of 4.4–7.4 μm with the geometric standard deviation ranging from 1.23 to 1.33. High-speed homogenization during droplet formation is useful for a reduction in the size of the prepared composite particles. In addition, the appropriate surfactant concentration has a significant effect on the particles' morphology. However, the concentration of the nanopigment did not significantly change either particle morphology or particle size. © 2008 Wiley Periodicals, Inc. J Appl Polym Sci 108: 1288–1297, 2008

Key words: composites; suspension polymerization; pigment; particle size distribution; toner

INTRODUCTION

Composite particles of polymers and pigment are of particular interest because of their potential use in paint, in toner for electrophotography printing,[1–3] in inks for ink-jet printing,[4,5] and in electronic ink for colored electrophoretic displays.[6–10] High-quality toner, or ink, is required to improve image quality. High-quality toner, or ink, is characterized by very small particle size with a narrow size distribution and a spherical morphology. Therefore, particle size, size distribution and morphology of toner particles and electronic inks are critical for the production of high-resolution images and to decrease edge roughness.[8,11,12] To produce composite particles of polymer and pigment with smaller particle size, narrow size distribution, and spherical morphology, process conditions, and concentration of involved materials must be optimized.

In the production of composite particles, including organic or inorganic particles within a polymer particle, size and morphology of the incorporated particles determines the geometrical (size and shape) and physical properties of the composite particles.[13] To produce high-quality pigment-polymer composite, high-quality pigment is required. The coloring properties of pigment, such as color strength, color shade, transparency, and flow properties, correlate well with pigment particle size and shape.[14] Nanopigments demonstrate outstanding performance due to their very small size. Nanopigments have the ability to pass through any blockage as a result of pseudosolution behavior, which is useful for printing processes.[15] Koo et al.[16,17] reports that nanopigments can enhance the visible light transmittance ratio as high as 100%, due to the ability to reduce light scattering in color filter application. Bermer[18] and Lee[19] demonstrated that nanopigments significantly influence image quality in ink-jet inks. Thus, nanopigments are required for the production of high-quality pigment-polymer composites.

To produce pigment-polymer composite particles, the chemical methods of polymerization and electrohydrodynamic atomization[20] are widely used. Polymerization methods, such as emulsion polymerization,[8,21] mini-emulsion polymerization,[22–25] and suspension polymerization[1,2,12] have been successful in producing

Correspondence to: K. Okuyama (okuyama@hiroshima-u.ac.jp).

Contract grant sponsors: the Ministry of Education, Culture, Sport, Science and Technology and Kumahira Scholarship Foundation.

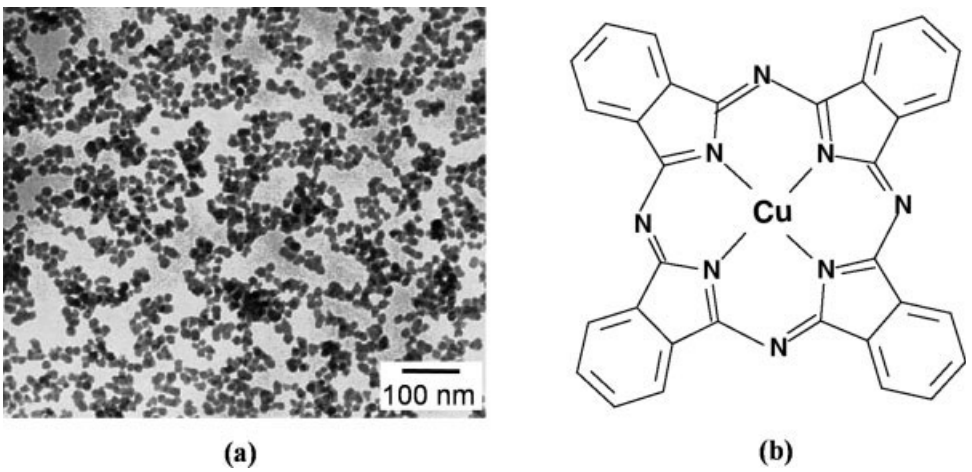

Figure 1 (a) Transmission electron microscopy image of nanoblue pigment. (b) Structure formulae of C.I. Pigment Blue (Copper Phthalocyanine blue: PB15 : 3).

pigment-polymer composite particles for widespread applications. Emulsion polymerization and mini-emulsion polymerization are general methods for producing stable latex with particle sizes on a submicrometer scale or smaller. Meanwhile, suspension polymerization is widely used to produce polymer composite beads ranging in sizes of from 10 to 1000 μm.[26,27] Compared with emulsion polymerization, suspension polymerization has the advantage of producing perfectly spherical composite polymer particles with less absorption of the stabilizer.[28,29] In suspension polymerization, bulk polymerization is carried out in the suspended droplets of monomers.[26] The final products are beads about the same size of the original monomer droplets. Therefore, the monomer droplet size is critical and significantly related to the particle size and particle size distribution of composite bead particles produced by suspension polymerization.[30]

In this study, we report on the production of relatively small (less than 10 μm) nanopigment-polymer composites with good geometrical properties using a new strategy of high-speed homogenization-assisted suspension polymerization. The prepared composite particles are nanopigment-poly(Styrene-*co*-*n*-butylacrylate-*co*-methacrylic acid) [poly(St-*co*-nBA-*co*-MAA)]. High-speed homogenization was used to reduce the size of monomer droplets. Nanosized hybrid blue pigment was used to produce high-quality composite particles. The effects of process parameters, i.e., speed of homogenizer agitation, surfactant concentration, and pigment concentration, on the morphology and particle size distribution of the prepared composite particles was determined.

EXPERIMENTAL

Materials

Styrene (St), *n*-butyl acrylate (*n*-BA), and methacrylic acid (MAA) monomers were reagent grade (all purchased from Kanto Chemical Co., Inc, Tokyo, Japan), and were distilled before use to remove the inhibitor. Divinyl benzene (DVB, Kanto Chemical, Co., Inc, Tokyo, Japan) was used as a crosslinking agent. 2,2′-Azobis(2,4-dimethyl-valeronitrile) (ADVN, Wako Pure Chemicals, Osaka, Japan) was used as a radical initiator for polymerization. Tricalcium phosphate (TCP, Kanto Chemical Co., Inc, Tokyo, Japan) and sodium dodecyl benzene sulfonate (NaDBS, Kanto Chemical Co., Inc, Tokyo, Japan) were used as a suspension stabilizer and surfactant, respectively. The hybrid blue pigment was provided by Toda Kogyo Co., Hiroshima, Japan. The pigment was in a core–shell structure with a silica particle in the core and organic pigment (copper phthalocyanine blue; C.I. Pigment blue15 : 3) in the shell.[15] Figure 1(a) shows a transmission electron microscopy image of the nanoblue pigment, which was approximately 18 nm in diameter. The nanopigment had a spherical shape and a narrow size distribution. The structural formulae of C.I. Pigment blue 15 : 3 is shown in Figure 1(b).

METHOD

Preparation of the composite particles of nanopigment-poly(St-*co*-nBA-*co*-MAA) by high speed homogenization-assisted suspension polymerization is shown schematically in Figure 2(a).[11] In an attempt to reduce the size of monomer droplets, high-speed homogenization was employed to assist droplet formation. The experimental method is described in detail in this section. The 20 g monomer mixture was composed of styrene (66.2 wt %), *n*-butylacrylate (28.3 wt %), MAA (5 wt %), and divinylebenzene (0.5 wt %), which was mixed with ADVN (2 wt % of total monomers). The nanopigment was added to the monomer mixture and premixed for 20 min at an agitation speed of 6500 rpm using homogenizer

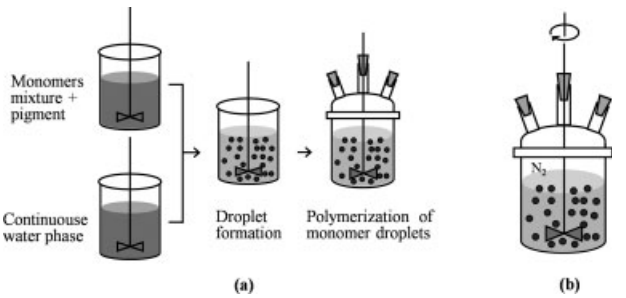

Figure 2 (a) Schematic diagram of experimental steps. (b) Schematic of basic stirred, jacketed batch reactor used for suspension polymerization.

(IKA, T25 Ultra Turrax, Germany) to form a dispersed monomer phase. The continuous water phase (200 mL) was prepared by the dissolution of 2 wt % water of TCP and 100–175 ppm water of NaDBS. A representative recipe is presented in Table I. The dispersed monomer phase was poured into the continuous water phase and stirred for 30 min with a high-speed homogenizer (varied from 9500 to 17,500 rpm) to assist the formation of monomer droplets. The suspension of monomer droplets was immediately introduced into a double-wall glass reactor (300 mL) with a thermostat, equipped with a paddle stirrer, four spaced baffles, a water-cooled reflux condenser, and a nitrogen inlet for polymerization. The experimental apparatus for suspension polymerization is shown in Figure 2(b). Polymerization of monomer droplets was carried out for 6 h at a polymerization temperature of 70°C under permanent agitation (200 rpm) in the presence of nitrogen bubbling. TCP was removed from the surface of the final product by adding 0.1*M* of hydrochloric acid to the polymer particles, stirring for 30 min, then filtering, and washing with pure water until the pH of the filtrate became neutral. Ultrasonication during the sample washing was needed to avoid particle agglomeration. Finally, the composite polymer particles were dried *in vacuo* at room temperature.

Characterizations

The size and morphology of the composite polymer particles produced were investigated using field emission-scanning electron microscopy (FE-SEM, *S*-5200, Hitachi Ltd, Japan). Prior to SEM imaging, particle samples were sputter-coated with palladium-platina.[20] Particle size distributions were determined by measuring the diameter of particles taken by FE-SEM.

A Fourier transform infrared spectrometer (FTIR, IR-Prestige 21, Shimadzu Co., Japan) was used to evaluate the resin composition of the composite particles. Potassium bromide (KBr, Kanto Chemical Co. Inc., Tokyo, Japan) was used to obtain the infrared spectra of solids and was particularly well suited to powdered samples. The KBr pellets were prepared by grinding the mixture of KBr and sample to reduce the particle size, using an agate mortar and compressing into a disc. The KBr pellets were analyzed using an IR spectrophotometer.

Thermal analysis was acquired using a TGA/DTA 6200, SII thermogravimetric analyzer from Seiko Instruments Inc., Japan. About 5 mg of the sample was placed into an aluminum crucible for measurement. The heating rate was adjusted to 10°C min^{-1} under 200 mL min^{-1} ambient air and the recorded temperature ranged from 25 to 550°C.

RESULTS AND DISCUSSION

In a suspension polymerization reactor, dispersion was produced by droplet breakage and coalescence. Droplet breakage mainly occurred in regions of high shear stress, or as a result of turbulent speed and pressure fluctuation along the surface of the droplet. Meanwhile, droplet coalescence was prevented by turbulent agitation and the presence of surface-active agents (surfactant).[31,32] Therefore, high agitation speed was expected to enhance the breakage rate and prevent the coalescence of monomer droplets. The results of these experiments demonstrated how each process parameter in suspension polymerization influences the particle size, morphology, and thermal properties of nanopigment-poly(St-*co*-nBA-*co*-MAA) composite particles.

TABLE I
Representative Recipe for Suspension Polymerization of Nanopigment-Poly(St-*co*-nBA-*co*-MAA) Composites

Ingredient	Amounts
Monomer[a]	
St	66.2 wt %
n-BA	28.3 wt %
MAA	5 wt %
Crosslinking agent	
DVB	0.5 wt %
Continuous phase[b]	
Water	200 mL
TCP	2 wt %
NaDBS[c]	100–175 ppm
Pigment[d]	
CS-C100Y	0.2–1 g
Initiator[e]	
ADVN	0.4 g

[a] Total weight of monomer is 20 g.
[b] Total volume of continuous phase is 200 mL.
[c] NaDBS concentration is varied from 100–175 ppm of the total continuous phase.
[d] The weight of the nanopigment was varied from 0.2 to 1 g.
[e] Weight of ADVN is 2 wt % of the total monomer base).

TABLE II
Influence of Different Agitation Speed of Homogenization on Particle Size

Sample	Monomer				Continuous Phase (mL)	Agitation Speed (rpm)	d_{pg}[a](μm)	σ[b]
	St (g)	*n*-BA (g)	MAA (g)	DVB (g)				
A-1	13.24	5.66	5	0.5	200	9500	7.39	1.23
A-2	13.24	5.66	5	0.5	200	13000	5.39	1.26
A-3	13.24	5.66	5	0.5	200	175000	4.38	1.33

[a] Geometric mean diameter.
[b] Geometric standard deviation.

Effect of agitation speed

The size growth model of bead suspension polymerization reported by Winslow and Matreyek[30] suggests that the particle size is mainly determined by the droplet size in the lower conversion stage and by the stability of the monomer/polymer droplets in the high-conversion stage. If the coalescence of monomer/polymer droplets is negligible during polymerization, the particle size distribution of the final product of composite particles can be approximated with the size distribution of monomer droplets. According to this assumption, the particle size distribution can be predicted by Hinze's theory,[33] which is based on the dynamic balance between breakage and coalescence of dispersed droplets and assumes that breakage in the turbulent fields may be caused by viscous shear forces. By assuming that the coalescence of dispersed droplets can be neglected by employing a stabilizer, the mean suspended droplet size can be estimated based on Kolmogroff's turbulence microscale theory[34]:

$$d = k_1(\sigma/\rho_c)^{3/5}\varepsilon^{-2/5} \quad (1)$$

From Eq. (1) it can be shown that mean monomer droplet size (d) is proportional to $\sigma^{3/5}$ (interface ten-

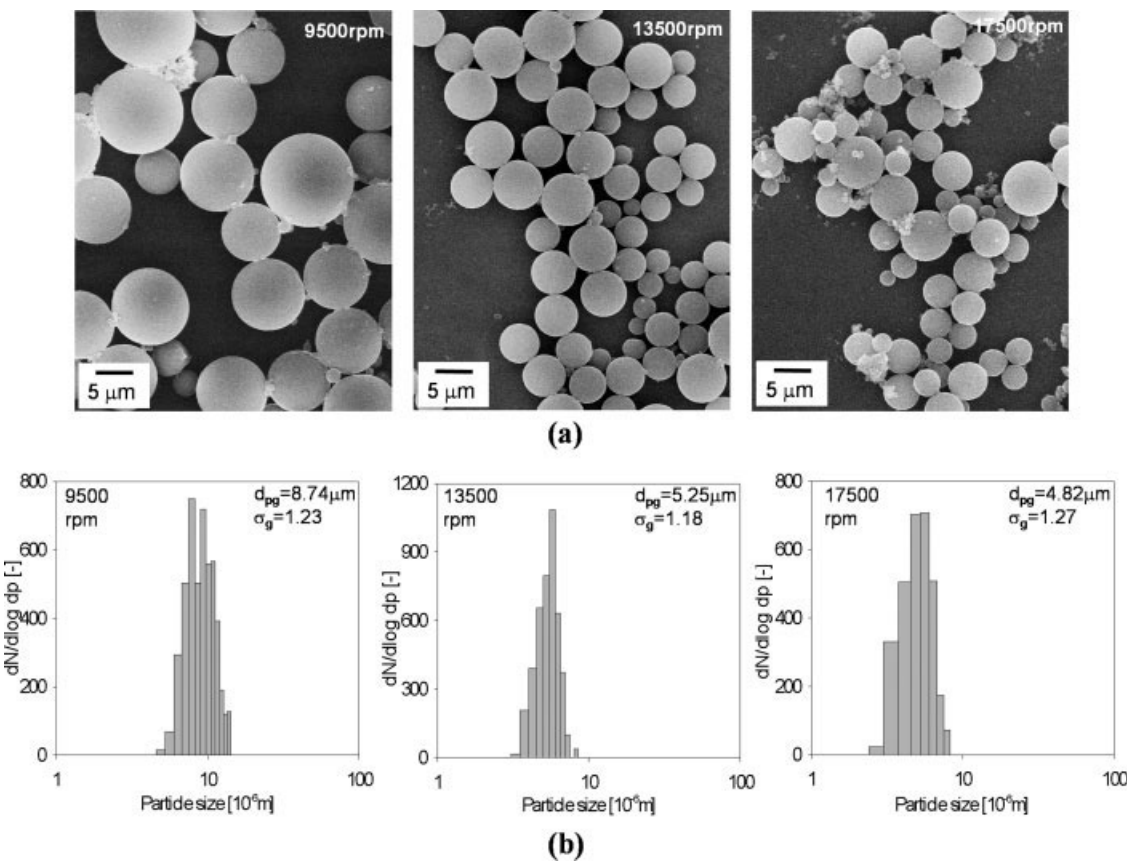

Figure 3 (a) Morphology of composite particles with different agitation speeds during droplet formation; 9500, 13,500, and 17,500 rpm. (b) Size distribution function of composite particles with different agitation speeds during droplet formation.

TABLE III
Influence of NaDBS Surfactant Concentration on Thermal Decomposition of Composite Particles

Sample	Monomer				Continuous Phase (mL)	NaDBS (ppm)	Pigment (g)	T_{onset}[a] (°C)	T_{max}[b] (°C)
	St (g)	*n*-BA (g)	MAA (g)	DVB (g)					
B-1	13.24	5.66	5	0.5	200	100	1	345	391.6
B-2	13.24	5.66	5	0.5	200	150	1	340	387.2
B-3	13.24	5.66	5	0.5	200	175	1	330	380.7

[a] Onset temperature.
[b] Maximum temperature at thermal decomposition.

sion), $\rho^{-3/5}$ (density of continuous phase), and $\epsilon^{-2/5}$ (power density). The power density is significantly correlated with the agitation speed in the stirring reactor.

$$\varepsilon \propto k_2 n^3 \tag{2}$$

where n is the agitation speed and k_2 is a coefficient related to the blade. Therefore eq. 1 can be expressed as eq. 3:

$$d = k_3(\sigma/\rho_c)^{3/5} n^{-6/5} \tag{3}$$

This equation is only valid for noncoalesced and nonincorporated particles within a polymer particle. However, this equation explains that the mean monomer droplet size is significantly correlated with agitation speed. The present experiment was carried out with agitation speeds varying from 9500 rpm to 17,500 rpm to assist the formation of monomer droplets. This is the highest speed reported for a suspension polymerization method.[11,27] The corresponding monomer composition data and operation conditions are given in Table II. The monomers, containing St/*n*-BA/MAA/DVB with weight ratio of 66.2/28.3/5/0.5, were used identically. An aqueous phase containing pure water and surfactant was used as the continuous phase and became the heat transfer medium.[26] NaDBS (100 ppm) was employed and adjusted for all samples (A-1, A-2, and A-3). In this case, the pigment was not incorporated into the monomer mixture.

Figure 3(a) shows the FE-SEM images of the prepared composite particles. The prepared composite particles exhibit a regular spherical shape, with diameter size decreased as agitation speed increases

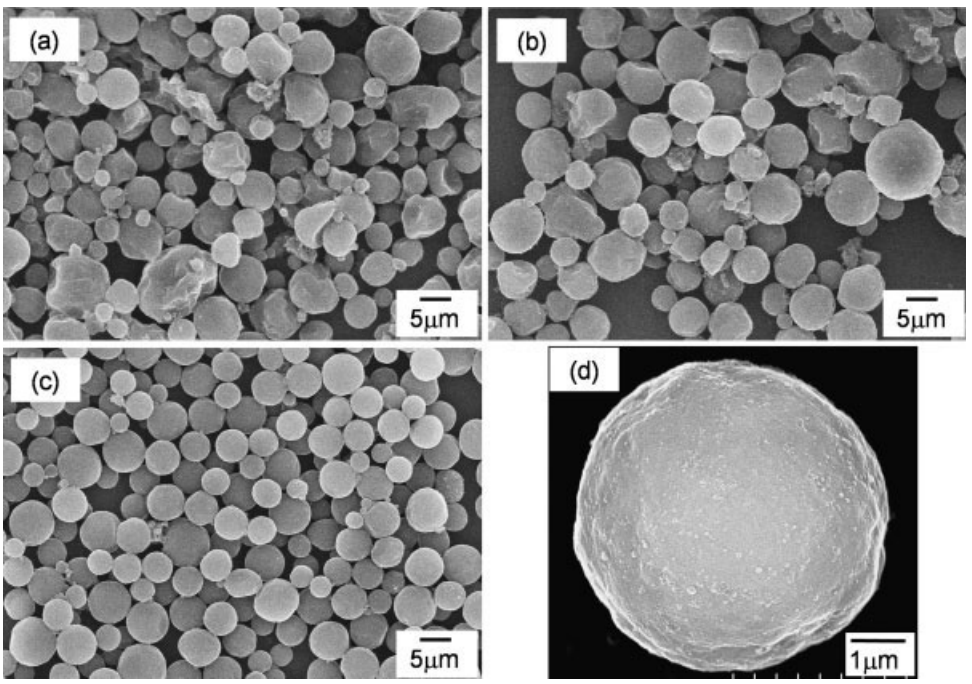

Figure 4 Morphology of composite particles as a function of NaDBS concentration (a) B-3, (b) B-2, (c) B-1 and (d) high magnification for sample B-1.

during monomer droplet formation. Figure 3(b) shows the size distribution of the composite particles produced by changing the agitation speeds during monomer droplet formation. The size distribution of composite particles followed a log-normal distribution with geometric mean diameters, d_{pg} of 8.74, 5.25, and 4.82 μm, for samples prepared with agitation speed of 9500, 13,500, and 17,500 rpm, respectively. The prepared composite particles exhibited a narrow size distribution with geometric standard deviation, σ_g, ranging from 1.18 to 1.27. When the formation of monomer droplets was carried out at 17,500 rpm of agitation speed, the mean size of the particles produced was significantly reduced. However, the size distribution function was slightly broader, with the geometric standard deviation, σ_g, at around 1.27. This result indicates that high agitation speed resulted in a significant reduction of the monomer droplet size,[35] which significantly correlated with the size of the final product composite particles.[26]

Effect of surfactant concentration

Surface-active agents (surfactant) are effective in reducing the interfacial tension between oil and water and in preventing droplet coalescence during suspension polymerization. The type and concentration of the surfactant are two of the process variables that determine the morphology properties of the polymer particles.[36] Sodium dodecyl benzene sulfonate (NaDBS), a type of anionic surfactant, was employed to produce composite particles of nanopigment-poly(St-*co*-nBA-*co*-MAA) to study the effect of surfactant concentration on thermal stability and on the morphology of the prepared composite particles. Table III provides the corresponding data, including morphology, and comparisons of thermal decomposition of composites produced by suspension polymerization with varied NaDBS concentrations. Figure 4 shows the FE-SEM images of the composite particles with different NaDBS concentrations. The NaDBS concentration has a significant effect on the morphology, or shape, of the composite particles. The results indicate that the asphericity of the composite particles of nanopigment-poly(St-*co*-nBA-*co*-MAA) increased with increasing NaDBS concentration (shown in Fig. 4). The sample B-1, which was prepared with 100 ppm of NaDBS from the total volume of the water-based continuous phase, produced spherical composite particles with geometric mean diameters, d_{pg} of approximately 4.55 μm [shown in Fig. 4(c,d)]. Figure 4(d) shows a higher magnification of sample B-1, which clearly shows that relatively spherical, dense composite particles could be produced. The surfaces of the composite particles are relatively smooth and the nanopigments blend well with the composite particles. The use of 150 and 175 ppm of NaDBS (samples B-2 and B-3) produced irregular shapes of composite particles [shown in Fig. 4(a,b)]. The polymerization was unsuccessful when the concentration of NaDBS exceeded 200 ppm of NaDBS (data not shown).

Generally in the suspension polymerization method, the initial monomer droplet shape largely determines the final shape of the composite polymer particle. Our previous research demonstrated that the structural stability of droplets have an important effect on particle morphology.[37] The structural stability of droplets can be explained by Bond's number β, the ratio of the inertial force and surface tension effects. The bond number is given by[38]

$$\beta = \left(\Delta\rho a d_d^2\right)\sigma^{-1} \tag{4}$$

where Δρ is the difference in the densities of droplets and surrounding fluid (for our case, the droplet is a

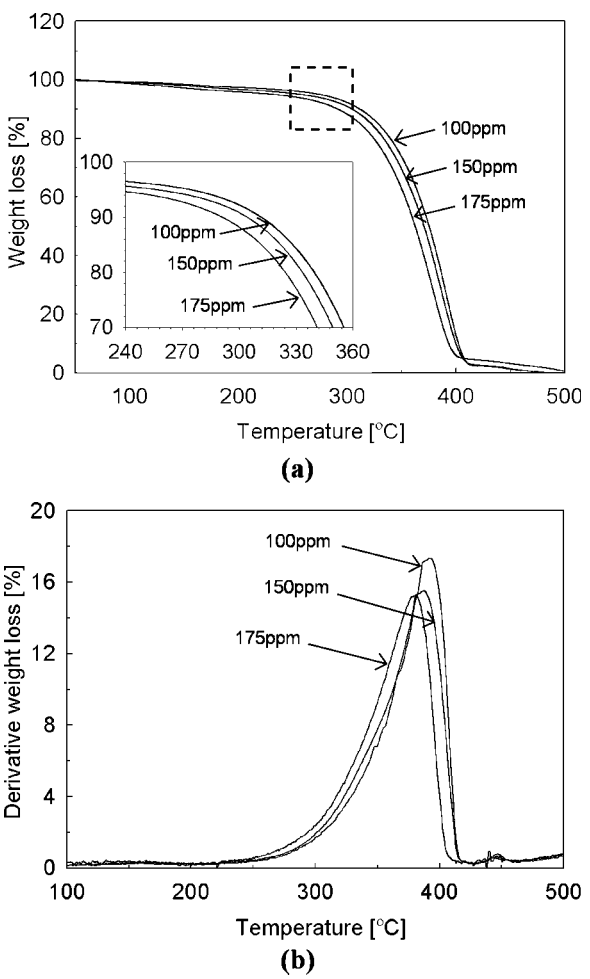

Figure 5 (a) TGA thermographs and (b) derivative weight loss of composite particles as a function of NaDBS concentration, 100, 150, and 175 ppm (Insert shows the variation in onset temperature).

TABLE IV
Influence on Particle Size of Incorporating Pigment Concentration

Sample	Monomer				Continuous Phase (mL)	NaDBS (g)[a]	Pigment (g)	d_{pg}[b] (μm)	σ[c]
	St (g)	*n*-BA (g)	MAA (g)	DVB (g)					
C-1	13.24	5.66	5	0.5	200	0.02	0	4.82	1.27
C-2	13.24	5.66	5	0.5	200	0.02	0.2	4.43	1.26
C-3	13.24	5.66	5	0.5	200	0.02	0.5	4.55	1.24
C-4	13.24	5.66	5	0.5	200	0.02	1	5.68	1.18

[a] NaDBS is 100 ppm from the total water based continuous phase.
[b] Geometric mean diameter.
[c] Geometric standard deviation.

monomer droplet and the surrounding fluid is water), a the acceleration associated with an inertial force, d_d the droplet size, and σ interfacial tension (strength of surface tension). The droplet is nearly spherical at values of $\beta \rightarrow 0$ and becomes flat when the value of β increases. Adding the surfactant into the water system reduces the σ value and imparts a β value increase. Although adding the surfactant prevents droplet coalescence, an inappropriate surfactant concentration results in a less stable droplet and an irregular composite polymer particle will be obtained. These results indicate that appropriate surfactant concentration is critical for the production of microsphere composite particles by suspension polymerization.

Figure 5 shows the TGA thermograph obtained from composite particles produced from different surfactant concentrations. The corresponding data are shown in Table III. The TGA curve shows no significant weight loss below 270°C. However, beyond this temperature the onset of degradation was notably influenced by the surfactant concentration in suspension polymerization. The maximum temperature of thermal decomposition shown by those composite particles shifted toward a higher temperature range with decreasing surfactant concentration [Fig. 4(b)]. This result indicates that a concentration of 100 ppm of NaDBS (sample B-1) produced composite particles of nanopigment-poly(St-*co*-nBA-*co*-MAA) with higher thermal stability than did concentrations of 150 and 175 ppm of NaDBS (sample B-2 and B-3). The FTIR analysis found no difference in bonding spectra among the samples (data not shown).

Effect of nanopigment blue concentration

Table IV shows the effect of nanopigment concentration on the prepared composite particles of nanopig-

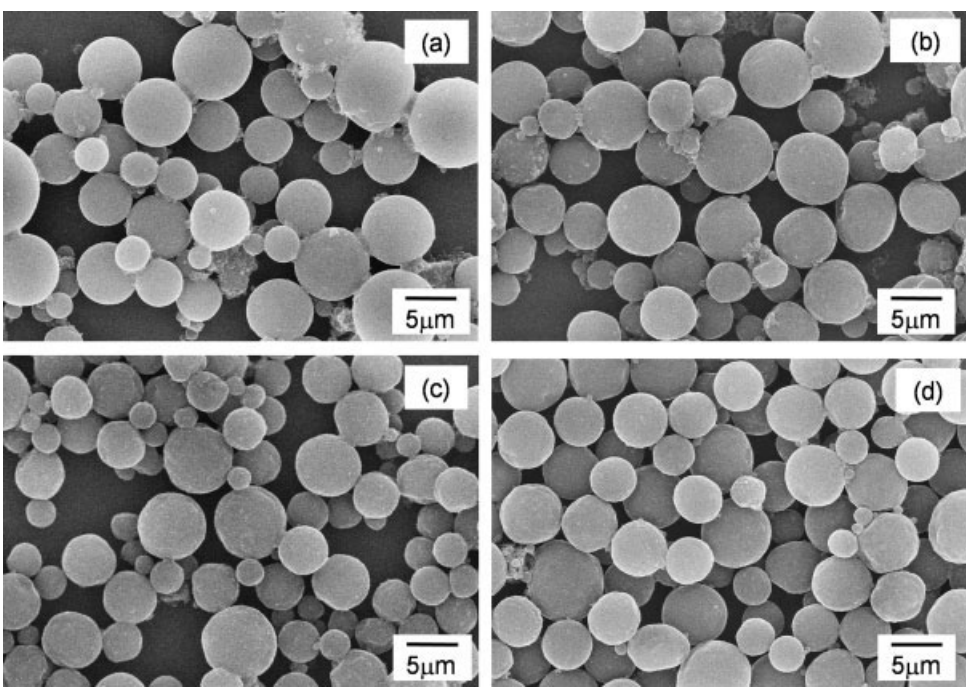

Figure 6 Morphology of composite particles as a function of pigment concentration (a) bare polymer C-1, (b) C-2, (c) C-3 and (d) C-4.

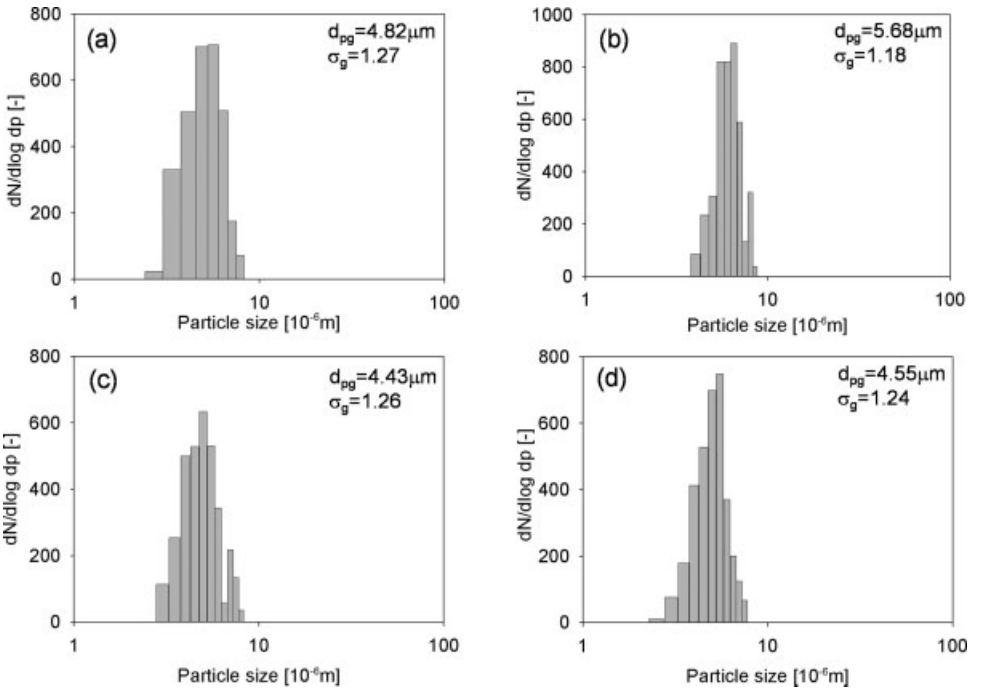

Figure 7 Size distribution functions of composite particles as a function of pigment concentration, (a) bare polymer C-1, (b) C-2, (c) C-3 and (d) C-4.

ment-poly(St-*co*-nBA-*co*-MAA). The weight ratio of monomers St/*n*-BA/MAA/DVB was 66.2/28.3/5/0.5 with NaDBS of 100 ppm identical for all composite particles produced. The operational conditions for monomer droplet formation were adjusted to an agitation speed of 17,500 rpm. Figure 6 shows FE-SEM images of composite particles produced by suspension polymerization with varying pigment concentrations (C-1, C-2, C-3, C-4). The results indicate that the amount of nanopigment concentration did not have a significant effect on either the morphology of the particles (Fig. 6) or on the geometric mean diameter, d_{pg}, of the particles (Fig. 7). Figure 7 shows the size distribution function of the bare poly(St-*co*-nBA-*co*-MAA) and pigment-poly(St-*co*-nBA-*co*-MAA) composite particles with varied incorporating pigment concentrations. A comparison of polymerization with and without the addition of nanopigment shows that the presence of pigment in the polymerization mixture did not significantly affect particle size. Figure 8 shows the geometric mean diameter, d_{pg}, as well as geometric standard deviation, σ_g, of the prepared composite particles. The particle size was not altered significantly with further increases made only in the weight of blue pigment from 0.2 to 1 g. The prepared composite particles had a narrow size distribution with a geometric standard deviation, σ_g, in the range of 1.18–1.27.

FTIR spectra results provided analysis of resin composition in the prepared composite nanopigment-poly (St-*co*-nBA-*co*-MAA). Figure 9 shows the FTIR spectra of nanopigment particles, bare polymer particles, poly (St-*co*-nBA-*co*-MAA) and three composite particles of nanopigment-poly(St-*co*-nBA-*co*-MAA) with different pigment concentrations. Figure 9(a) corresponds to the hybrid nanopigment showing the pigment had absorption bands at 1100 cm^{-1} (silica group),[39] 730 and 754 cm^{-1}. The bare poly (St-*co*-nBA-*co*-MAA) [Fig. 9(b)] had absorption bands at 3084, 3061, and 3026 cm^{-1} (aromatic C—H stretching); 2956 and 2870 cm^{-1} (aliphatic C—H stretching); 1730 cm^{-1} (C=O stretching of ester

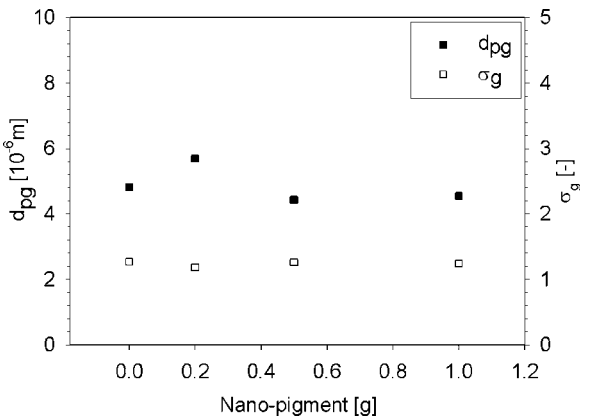

Figure 8 Geometric mean diameter and geometric standard deviation of composite particles of nanopigment-poly (St-*co*-nBA-*co*-MAA) with varied incorporation pigment concentrations.

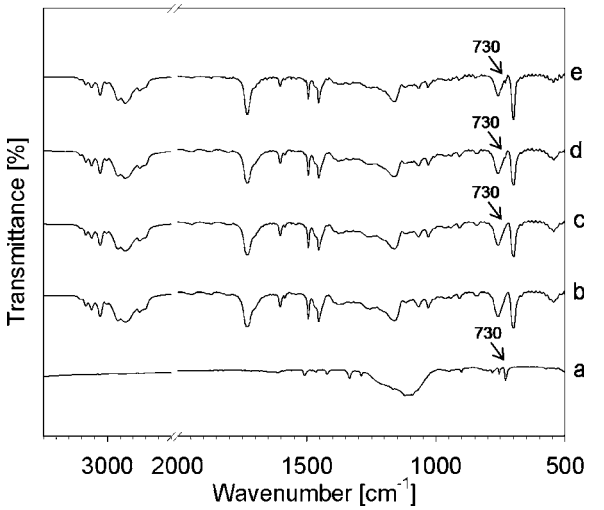

Figure 9 FTIR spectra of composite particles for different incorporated pigment concentrations (a) nanoblue pigment, (b) bare polymer C-1, (c) C-2, (d) C-3 and (e) C-4.

group in BA); 1602 cm^{-1} (C=C double bond of phenyl group in St) and 1703 cm^{-1} (C=O stretching of carboxyl group in MAA).[11] Figure 9(c–e) shows the composite particles of pigment-poly (St-*co*-nBA-*co*-MAA). In the spectra of Figure 9(c–e), the functional group was observed through the presence of band regions at 3084, 3061, and 3026 cm^{-1} (aromatic C—H stretching); 2956 and 2870 cm^{-1} (aliphatic C—H stretching); 1730 cm^{-1} (C=O stretching of ester group in BA); 1602 cm^{-1} (C=C double bond of phenyl group in St) and 1703 cm^{-1} (C=O stretching of carboxyl group in MAA). In addition, the peaks at 730 cm^{-1} (strong) and 754 cm^{-1} (medium) were observed in the spectrum shown in Figure 9(c–e). These peaks indicate that pigment was incorporated within the composites particles. The intensity of the peak at 730 cm^{-1} clearly increases with increasing nanopigment concentration within composites particle. These FTIR spectra results prove the formation of composite particles.

CONCLUSIONS

Nanoblue pigment-poly(St-*co*-nBA-*co*-MAA) composite particles were successfully prepared by high-speed homogenization-assisted suspension polymerization. The prepared composite particles had a regular microspherical morphology with a narrow size distribution (geometric standard deviations in the range of 1.18–1.27). High-speed homogenization resulted in the formation of smaller monomer droplets, which correlates with the production of smaller composites of pigment-polymer particles. NaDBS was employed as a surfactant for suspension polymerization; the appropriate NaDBS concentration is necessary for the obtainment of composite particles with a spherical morphology. The TGA results indicate the temperature of thermal decomposition increased slightly with decreasing surfactant concentration. The nanopigment concentration had no significant effect on either morphology or particle size of the prepared composite particles.

The authors thank Toda Kogyo Corp. (Hiroshima) for providing the nanopigment particles.

References

1. Yang, J.; Wang, T. J.; He, H.; Wei, F.; Jin, Y. Ind Eng Chem Res 2003, 42, 5568.
2. Bakhshaee, M.; Pethrick, R. A.; Rashid, H.; Sherrington, D. C. Polymer 1985, 26, 185.
3. Hasegawa, J.; Yanagida, N.; Tamura, M. Colloids Surf A 1999, 153, 215.
4. Spinelli, H. J Adv Mater 1998, 10, 1215.
5. Xue, C. H.; Shi, M. M.; Chen, H. Z.; Wu, G.; Wang, M. Colloids Surf A 2006, 287, 147.
6. Kim, C. A.; Joung, M. J.; Ahn, S. D.; Kim, G. H.; Kang, S. Y.; You, I. K.; Oh, J.; Myoung, H. J.; Baek, K. H.; Suh, K. S. Synth Met 2005, 151, 181.
7. Kim, K. S.; Lee, J. Y.; Park, B. J.; Sung, J. H.; Chin, I.; Choi, H. J.; Lee, J. H. Colloid Polym Sci 2006, 284, 813.
8. Yu, D. G.; An, J. H.; Bae, J. Y.; Jung, D. J.; Kim, S.; Ahn, S. D.; Kang, S. Y.; Suh, K. S. Chem Mater 2004, 16, 4693.
9. Yu, D. G.; An, J. H. J Polym Sci Part A: Polym Chem 2004, 42, 5608.
10. Comiskey, B.; Albert, J. D.; Yoshizawa, H.; Jacobson, J. Nature 1998, 394, 253.
11. Sawatari, N.; Fukuda, M.; Taguchi, Y.; Tanaka, M. J Appl Polym Sci 2005, 97, 682.
12. Kiatkamjornwong, S.; Pomsanam, P. J Appl Polym Sci 2003, 89, 238.
13. Jose, M. V.; Dean, D.; Tyner, J.; Price, G.; Nyairo, E. J Appl Polym Sci 2007, 103, 3844.
14. Horn, D.; Rieger, J. Angew Chem Int Ed 2001, 40, 4331.
15. Hayashi, K.; Morii, H.; Iwasaki, K.; Horie, S.; Horiishi, N.; Ichimura, K. J Mater Chem 2007, 17, 527.
16. Koo, H. S.; Pan, P. C.; Kawai, T.; Chen, M.; Wu, F. M.; Liu, Y. T.; Chang, S. J Appl Phys Lett 2006, 88, 111908
17. Koo, H. S.; Chen, M.; Pan, P. C.; Chou, L. T.; Wu, F. M.; Chan, S. J.; Kawai, T. Displays 2006, 27, 124.
18. Bermel, A. D.; Bugner, D. E. J Imaging Sci Technol 1999, 43, 320.
19. Lee, H. K.; Joyce, M. K.; Fleming, P. D. J Imaging Sci Technol 2005, 49, 54.
20. Widiyandari, H.; Jr., Hogan, C. J.; Yun, K. M.; Iskandar, F.; Biswas, P.; Okuyama, K. Macromol Mater Eng 2007, 292, 495.
21. Yu, D. G.; An, J. H.; Bae, J. Y.; Ahn, S. D.; Kang, S. Y.; Suh, K. S. J Appl Polym Sci 2005, 97, 72.
22. Lelu, S.; Novat, C.; Graillat, C.; Guyot, A.; Bourgeat-Lami, E. Polym Int 2003, 52, 542.
23. Tiarks, F.; Landfester, K.; Anonietti, M. Macromol Chem Phys 2001, 202, 51.
24. Al-Ghamdi, G. H.; Sudol, E. D.; Dimonie, V. L.; El-Aasser, M. S. J Appl Polym Sci 2006, 101, 3479.
25. Erdem, B.; Sudol, E. D.; Dimonie, V. L.; El-Aasser, M. S. J Polym Sci Part A: Polym Chem 2000, 38, 4431.
26. Rodriguez, F.; Cohen, C.; Ober, C. K.; Archer, L. A. Principles of Polymer Systems, 5th ed.; Taylor & Francis: New York, 2003.
27. Ramirez, J. C.; Herrera-Ordonez, J.; Gonzalez, V. A. Polymer 2006, 47, 3336.

28. Yuan, H. G.; Kalfas, G.; Ray, W. H. J. Macromol Sci Rev Macromol Chem Phys 1991, C31, 215.
29. Vivaldo-Lima, E.; Wood, P. E.; Hamielec, A. E.; Penlidis, A. Ind Eng Chem Res 1997, 36, 939.
30. Winslow, F. H.; Matreyek, W. Ind Eng Chem 1951, 43, 108.
31. Chatzi, E. G.; Kiparissides, C. Chem Eng Sci 1994, 49, 5039.
32. Chatzi, E. G.; Kiparissides, C. AIChE J 1995, 41, 1640.
33. Hinze, J. O. AIChE J 1955, 1, 289.
34. Coulaloglou, C. A.; Tavlarides, L. L. Chem Eng Sci 1977, 32, 1289.
35. Alexandridou, S.; Kiparissides, C. J Microencapsulation 1994, 11, 603.
36. Alexopoulos, A. H.; Kiparissides, C. Chem Eng Sci 2007, 62, 3970.
37. Iskandar, F.; Gradon, L.; Okuyama, K. J Colloid Interface Sci 2003, 265, 296.
38. Velev, O. D.; Lenhoff, A. M.; Kaler, E. W. Science 2000, 287, 2240.
39. Colthup, N. B.; Daly, L. H.; Wiberley, S. E. Introduction to infrared and Raman Spectroscopy, 3rd ed.; Academic Press: Boston, 1990.